Proceedings of ICAR 2003 pp 726-732
The 11th International Conference on Advanced Robotics
Coimbra, Portugal, June 30 - July 3, 2003

ICAR Outstanding Paper Award

OSCAR and OCTAVE : Two bio-inspired visually guided aerial micro-robots

F. Ruffier S. Viollet N. Franceschini

Biorobotics Research Group, Movement and Perception Lab., CNRS/Univ. de la Méditerranée,
31, chemin Joseph Aiguier, 13402 Marseille Cedex 20, FRANCE
{ruffier, viollet, franceschini}@laps.univ-mrs.fr

Abstract

In the framework of our research on biologically inspired microrobotics, we have developed two novel Automatic Flight Control Systems (AFCS): OCTAVE (Optical altitude Control sysTem for Autonomous VEhicles) and OSCAR (Optical Scanning sensor for the Control of Autonomous Robots), both based on insects' visuomotor control systems. OCTAVE was tested and found to confer on a tethered aerial robot (the OCTAVE robot) the ability to perform terrain following. OSCAR gives a tethered aerial robot (the OSCAR robot) the ability to fixate and track a contrasting target with a high level of accuracy. Both OCTAVE and OSCAR robots are based on optical velocity sensors, the principle of which was based on previous electrophysiological studies on the fly's Elementary Motion Detector (EMD) neurons performed at our laboratory. Both processing systems described are light enough to be mounted on-board Micro-Air-Vehicles (MAV) with an avionic payload small enough to be expressed in grams rather than kilograms.

1. Introduction

The biorobotic approach we have been using at our laboratory since 1985 has led to designing, simulating and constructing biologically inspired visual sensors and complete visuomotor control systems. Transferring biological principles to smart machines (robots) can provide solutions to the problems arising when implementing complex behavior (obstacle avoidance, hovering, Nap-Of-the-Earth flight,…) in Micro-Air Vehicles (MAVs) while yielding some fruitful returns to biology [1-10].

Present-day research on Micro-Air Vehicles with very small dimensions in the 10-50cm range has come up against a serious problem: how to confer on micro aircraft some authority and autonomy in spite of the severe energy and mass constraints involved. Short range observation missions require skills such as coping with variations in ground relief or tracking a target. In the most sophisticated Unmanned Air Vehicles (UAV) and Micro Air Vehicles (MAV) or micro-drones, the eyes and brain of the human pilot have to be replaced by an on-board processing system capable of steering the aircraft through even the most cluttered environments. This problem has been solved for hundred million years by winged insects. These are highly evolved autonomous flying machines that can serve as useful models for designing the MAVs of the future. Thus far only few studies have attempted to draw on these models to perform visual guidance of flying robots [3, 6, 8, 11-15]. Natural MAVs display remarkable visuomotor behavior with few pixels (approximately 10^3) in their eyes and few neurons (approximately 10^6) in their brains as compared with humans. Behavioral experiments have shown that flying insects' stabilization and guidance depend on the speed at which the contrasting features they encounter slide across their retina (this has been called the retinal slip speed or the optic flow) [16]. Winged insects extract the relevant information from the optic flow by using particular neurons called Elementary Motion Detectors (EMDs) [17-18]. In 1986, Franceschini and al. built a biomimetic velocity sensor using discrete electronics to estimate the directional optic flow [19]. The principle of this sensor was based on the findings on fly EMDs, obtained at our laboratory by recording from single neurons while concomitantly stimulating single photoreceptor cells on the retinal mosaic [20].

All our robots have been equipped with these EMD circuits that estimate the directional optic flow. The EMD circuit of the OCTAVE system (Optical altitude Control sysTem for Autonomous VEhicles) responds to the relative motion of an aerial vehicle with respect to the contrasting terrain underneath. The OCTAVE Automatic Flight Control System (AFCS) presented here draws on a hypothesis put forward 50 years ago [21], according to which flying locusts would have a preferred retinal velocity. We show here that the OCTAVE robot can drive its lift automatically so as to follow a terrain over a wide range of ground speeds, by relying essentially on the data provided by an EMD sensor oriented downwards.

By contrast, the OSCAR sensor (Optical Scanning sensor for the Control of Autonomous Robots) responds to micro-scanning movements imposed on the visual sensor itself. The particular movement imposed on the OSCAR eye is largely based on the retinal micro-scanning system described in the flying fly [22]. Upon simulating an elementary scanning eye placed in a simple visual environment, we established that micro-scanning plus motion detection systems can be used for both detecting and locating targets to an accuracy of a fraction of a pixel period [5].

In section 2, we describe the EMD circuit, which is a basic component of both the OCTAVE and OSCAR robots. In section 3, we outline the OCTAVE control system and show some results on terrain following. In section 4, we describe the principle, design, construction and calibration of the OSCAR sensor. We illustrate its capacities on board the OSCAR robot, which is a miniature twin-engine rotorcraft that is able to stabilize around its yaw axis and track a moving target with great accuracy.

2. Visual motion processing

Both the OCTAVE and OSCAR visual processing systems rely on the same eye and on the same electronic Elementary Motion Detector (EMD) (Figure 1).

The elementary retina consists of only two photoreceptors Ph1 and Ph2, the visual axes of which are separated by an interreceptor angle $\Delta\varphi = 4°$ (Figure 1a) – a value close to that between adjacent facets in the fruitfly eye [23]. The retina is deliberately defocused until the Field Of View (FOV) of each photoreceptor (angular sensitivity function) becomes Gaussian-like, so that it acts as an adequate spatial low pass filter [23].

The relative angular speed Ω of a contrasting feature in the environment ("optic flow") is measured according to the following definition :

$$\Omega = \frac{\Delta\varphi}{\Delta t} \qquad (1)$$

where Δt is the time taken by a contrasting edge to cross both optical axes successively (Figure 1b). The angular speed Ω results either from a translational motion (as occurs on the OCTAVE robot) or from a rotational motion (as imposed on the OSCAR's eye). The original EMD scheme [19] consists of several processing steps (Figure 1c) :

1. Band-pass temporal filtering on each channel.
2. Thresholding and pulse generation on each channel.
3. Generating a long-lived decaying signal on one channel.
4. Generating a very short, unitary sampling pulse on the other channel.
5. Minimum-detection based sampling on the second channel delivers a signal that decreases monotonically with Δt (and hence increases with Ω).

Our current hybrid (analog + digital) implementation of an EMD is a small module weighing only 0.8 grams and consuming 40mW [9].

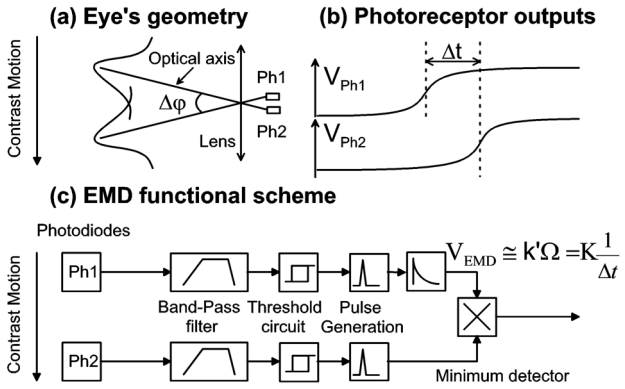

Figure 1. (a) The eye consists of a lens and 2 photoreceptors, the visual axes of which are separated by an angle $\Delta\varphi$. The lens (diameter 5mm, focal length 8.5mm) mounted in front of the silicon PIN photodiodes is defocused until their angular sensitivity becomes bell-shaped. **(b)** Rotational or translational movement of this eye in front of a stationary contrasting feature generates a delay Δt between the two photoreceptor signals. **(c)** Block diagram of the EMD circuit consisting of several linear and nonlinear processing steps.

3. OCTAVE : a bio-inspired flight control system

3.1. The OCTAVE principle

Let us imagine a MAV flying in pure translation over an unknown terrain. As viewed from the aircraft vertically downwards (Fig 3a.), the angular slip speed Ω – the optic flow – is given by :

$$\Omega = \frac{v_x}{h} \qquad (2)$$

where v_x is the ground speed of the aircraft and h its local altitude over the terrain. This formula means that even in this most simple case of optic flow generated by a a self translation, the optic flow depends jointly on ground speed and altitude.

In the OCTAVE system, any variations in the optic flow measured downwards are assumed to be caused by variations in the height h above the ground. The OCTAVE visuomotor control loop [10] then acts so as to servo the optic flow Ω to a reference value at any time by driving the lift force continuously. As a result, the micro-flyer

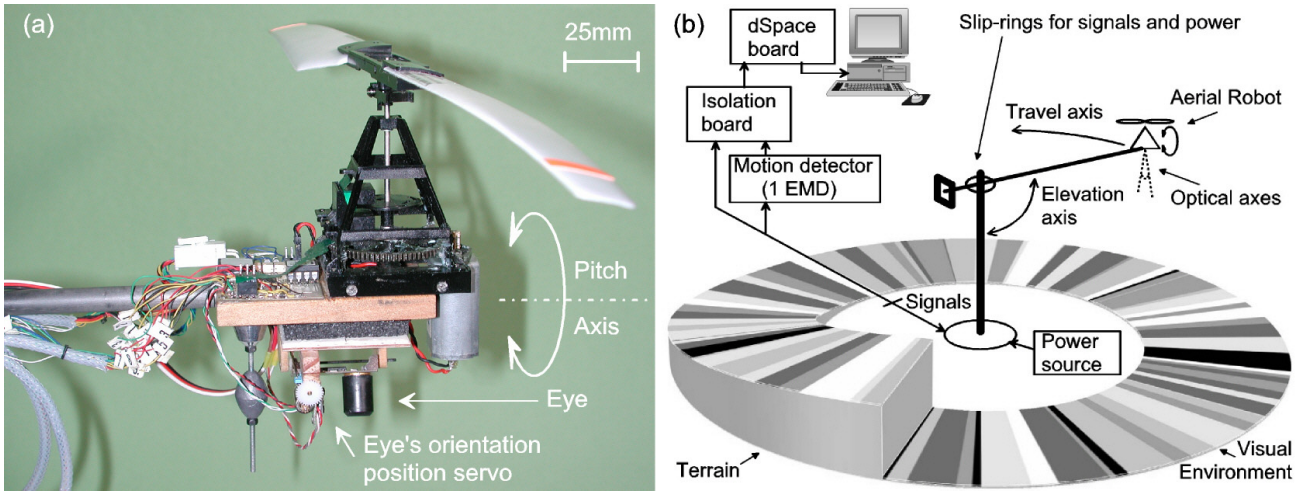

Figure 2. (a) The 100-gram MAV is equipped with a fixed-pitch rotor (extracted from a Keyence Revolutor micro-helicopter), a two-pixels eye and an onboard electronic processing system. **(b)** Test-rig composed of a pantographic whirling arm [7] and a 4.5-meter diameter disc onto which a texture consisting of randomly distributed, variously contrasting sectors was printed (edge contrast ***m*** ranging from 4% to 30%). The printed disc is placed on a circular ramp used as the relief.

attempts to maintain a height ***h*** above ground – a height which is automatically scaled by its speed. It therefore rises and descends, according to the underlying terrain.

3.2. Experimental setup

We built a small rotorcraft consisting of a motor driving a single fixed pitch propeller via a reduction gear (Figure 2a). The motor is controlled by Pulse Width Modulation (PWM); its speed (*rpm*) is measured by an on-board optronic sensor and servoed to the reference value dictated by the visuo-motor control system.

A balanced pantographic whirling arm [7] allows the tethered MAV to lift itself and move in azimuth and elevation around a central pole (Figure 2b) above a richly patterned "terrain". The 100-gram rotorcraft is mounted on the axis of a position servo system located at the end of the whirling arm, which makes it possible for the experimenter to remotely set the robot's pitch angle (Figure 3a) and thus the horizontal speed ***v***. The advantage of this experimental rig is that it enables us to keep the minimum number of degrees of freedom, while testing the basic visuo-motor principles reliably and reproducibly, and monitoring a large number of parameters simultaneously. The width of the contrasting sectors (which ranged from 1cm to 30cm) and their grey levels were chosen at random in order to test the invariance of the processing system to the characteristics of the contrasting features encountered in the environment. The effective contrast ***m*** between any two edges ranges from 4% to 30%.

A computer equipped with a dSpace DSP board with analog I/O connected to a Matlab/Simulink software environment calculated the desired rotor *rpm* of the MAV, while monitoring various parameters such as the speed of travel, the altitude, the pitch angle, the rotor speed and the EMD output. All these signals were transmitted to or from the computer via a miniature slip-ring assembly.

When the robot is pitched forward, its eye automatically counterrotates to keep aiming downwards ($\varphi = 90°$ in Figure 3a). Eye counterrotation is achieved by an onboard 2.4 gram microservo (Figure 2a).

The EMD picks out the horizontal component of the optic flow. At this stage, the EMD circuit described in section 2 was placed off-board to assess **Ω**.

3.3. Terrain following results with OCTAVE

To test the automatic terrain-following abilities of the robot based on the use of optic flow, we placed one third (i.e., an approximately 4-meter portion) of the annular pattern on a sloping plane (the "circular ramp": Figure 2b). The result was that the OCTAVE visuomotor control loop controlled the rotor *rpm* in such a way that the robot's altitude varied automatically according to the changes in the relief of the land (Figure 3b). During these terrain following tests, the horizontal ground speed component happened to be maintained at a relatively constant value (Figure 3c). The automatic altitude control system is robust and efficient over a wide range of ground speeds (1 to 3 m/s in Figure 3c) and does not need to be trimmed to any particular ground speed.

The higher the speed at which the helicopter is flying, the higher its altitude will be. The avoidance which occurs when the robot is rising above the upward ramp (Figure 3b) is less pronounced at high flying speeds (curve n°4 ≈ 3 m/s) than at low speeds (curve n°1 ≈ 1 m/s). A "safe altitude" is thus automatically generated, which increases suitably with the flying speed. These results show that the

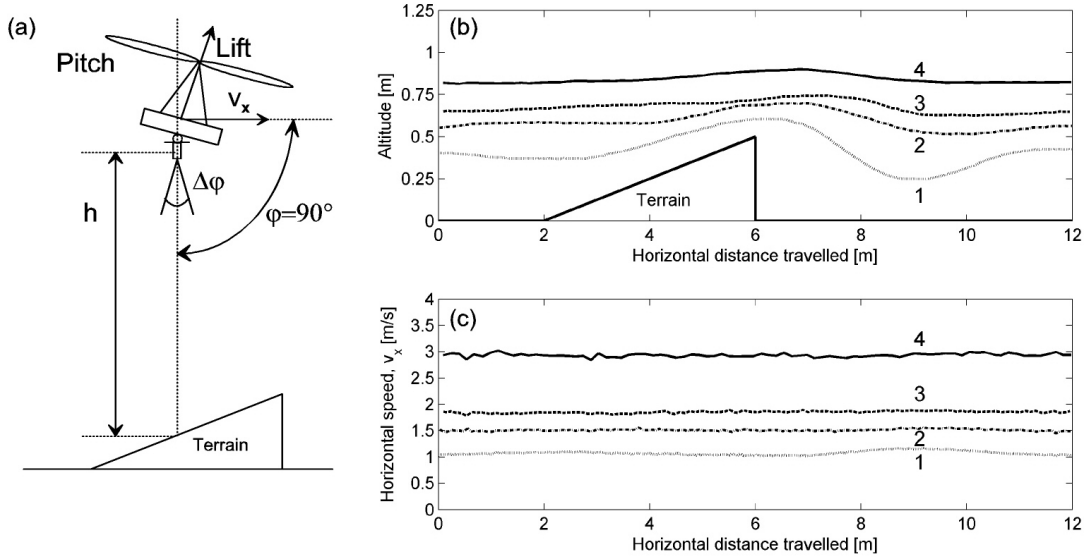

Figure 3. (a) The gaze direction is kept vertical whatever the aircraft pitch angle. **(b)** The OCTAVE system makes the robot follow the slanted terrain. The resulting trajectory depends on the horizontal ground speed of the aircraft: the faster it is traveling, the greater its altitude will be. **(c)** The ground speed can be seen to have remained constant in each of the four cases studied.

robot is able to follow the terrain reliably despite changes in the relief. Most importantly, this behavior is achieved *although no information about the actual value of the altitude or groundspeed is ever available on-board*. The flight trajectories obtained were highly reproducible during several minutes despite the presence of aerodynamic disturbances such as ground effects and air turbulence (Figure 4).

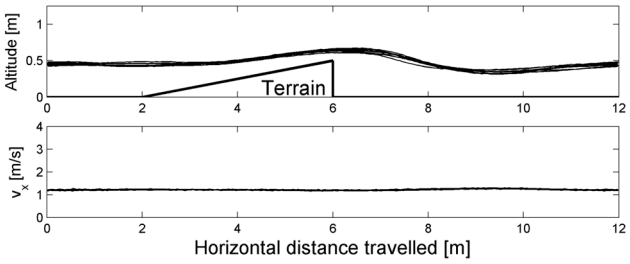

Figure 4. Ten consecutive trajectories, during which the robot travelled a distance of 120m in 100 seconds without crashing, show the reproducibility and reliability of the OCTAVE visuomotor control system in the context of a terrain following test (horizontal speed is here 1.2m/s).

4. OSCAR : a bio-inspired scanning sensor

4.1. The OSCAR principle

In the OCTAVE robot described above, the visual sensor measured the relative angular speed **Ω** resulting from the robot's *pure translation* at a constant speed ***v***. By contrast, the OSCAR sensor generates a *pure rotation*, the peculiarity of which is that it varies with time (variable speed scanning).

Again the two photoreceptors are separated by an interreceptor angle $\Delta\varphi = 4°$ (Figure 5). In a previous study [5], we simulated the concerted rotation of two photoreceptors, Ph1 and Ph2, placed in front of an edge. The pair of photoreceptors was assumed to rotate first at a constant angular speed **Ω**, then at a speed which decayed exponentially with time, according to:

$$\Omega(t) = \frac{A}{\tau}\exp\left(-\frac{t}{\tau}\right) \qquad (3)$$

where A is the amplitude of scan and τ a time constant.

In these latter conditions, the output signal from an EMD circuit connected to the photoreceptors will depend only on the instant when **Ω** is measured. The key point is that this instant depends directly on the angular position (e.g., positions 1, 2, 3 in Figure 5) of the contrasting target (here an edge) placed in the visual field. In other words, the value of the measured *speed* **Ω** will be modulated by the angular *position* of the target in the sensor field of view. It is on this basis that we designed a sensor which, in its most elementary form, is driven by a single pair of photoreceptors that scan the environment periodically with a low amplitude and at a variable angular speed while driving an EMD circuit [5].

4.2. Description of the OSCAR sensor

We built a miniature scanner, the components of which

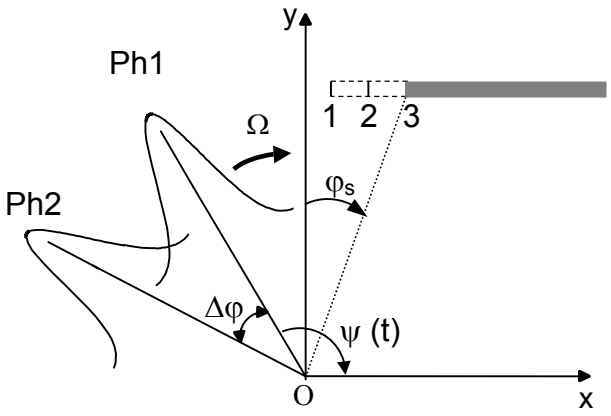

Figure 5. Sketch of two adjacent photoreceptors, Ph1 and Ph2, separated by a constant angle $\Delta\varphi$, which rotate clockwise at a variable angular speed Ω and encounter a dark edge placed here at arbitrary angular positions φ_s (1, 2, 3).

are shown in Figure 6a. A dual photosensor and a lens, mounted opposite each other on a blackened perspex drum (diameter 15mm), form a miniature "camera eye", which is rotated back and forth at 10Hz through a small angle α = 9° by a DC micromotor (diameter 10mm) with a reduction gear. The two photoreceptors of this "wiggling eye" are connected to an EMD via soft microwires.

The periodic scanning movement of the eye is generated through an accessory position servo-loop which controls the orientation of the eye-drum (and hence, that of the mean sensor's line of sight). The latter is monitored by a magnetoresistive sensor responding to the angular position of a micromagnet glued to the hub of the drum. A particular periodic input reference at 10 Hz is applied to the servo-loop so that the eye faithfully performs two imposed scan phases:

1. during the first phase (lasting 50ms), the angular speed Ω of the eye decreases quasi-exponentially,
2. during the second phase (lasting also 50ms), the eye returns to its original position at a constant speed.

4.3. Characteristics of the OSCAR sensor

We characterized the complete OSCAR scanning sensor by rotating it stepwise in front of a fixed target (an edge or a bar) while monitoring the response produced at each azimuthal orientation. Figures 6b shows an example of the sensor statical characteristics curves obtained with edges and a bar. The responses happen to be monotonic functions of the relative azimuthal orientation φ_s of the sensor. They are practically insensitive to the contrast (figure 6b) down to m = 0.12. At a distance of 200cm, however, the 1cm wide bar was detected only when the highest contrast (m = 0.85) was used (figure 6b). Remarkably, this bar subtended an angle (0.28°) which is 14 times smaller than the pixel period ($\Delta\varphi$ = 4°). Hence OSCAR *minimum visibile* is as fine as 7% of $\Delta\varphi$. In addition, the angular accuracy of the sensor in locating an edge or a bar is even better: approximately 0.1°, which represents only 2,5% of $\Delta\varphi$. OSCAR can therefore be said to have *hyperacuity* in spite of its minimalist number of pixels [24].

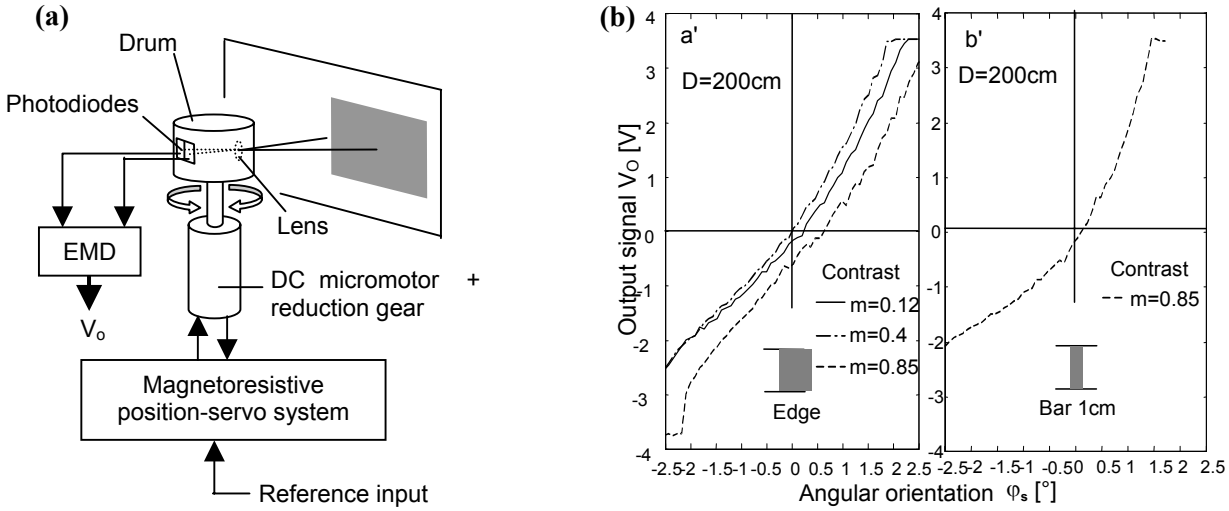

Figure 6. (a) Sketch of the complete OSCAR sensor in front of a dark bar posted up on the wall. The scanning law (exponential) is achieved by a position feedback loop where the sensor is a non contact magnetoresistive sensor. **(b)** Voltage output V_o from the OSCAR sensor as a function of its azimuthal orientation φ_s with respect to an edge (a') or a bar (b'). The angular range (± 2,5°) of φ_s was covered by applying successive micro-steps of 0,09°. Distance from the object D = 200cm. The parameter is the edge contrast m. Illuminance : 300 Lux.

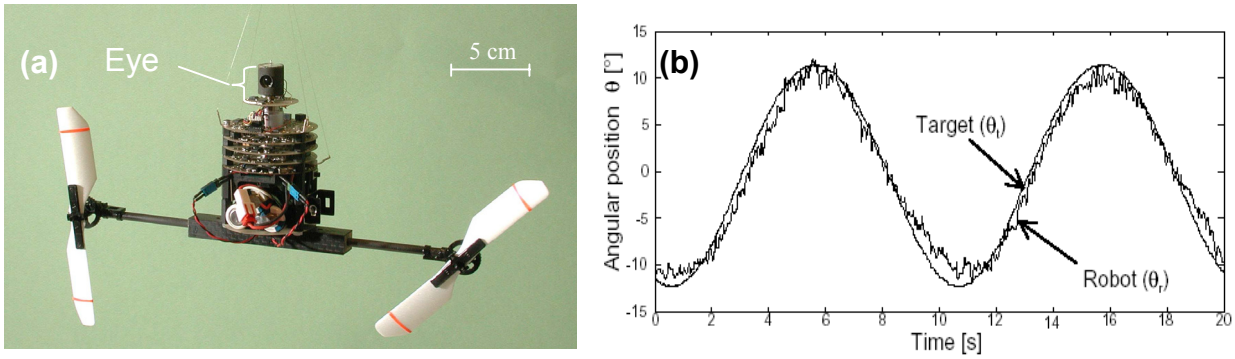

Figure 7. (a) Twin-engine OSCAR microrobot tethered to the ceiling. The robot orients about its yaw axis visually by making use of the OSCAR visual sensor (Figure 6). It controls the rotor speed of the two propellers differentially. It performs visual fixation, which leads to stabilization in a stationary environment or tracking, even in the presence of pendulum oscillations. The robot's heading direction is the same as the mean eye axis. **(b)** Visual tracking of a grey edge (contrast $\boldsymbol{m}$ = 0.4) by the micro aerial robot equipped with its OSCAR sensor. The "target" is an edge that was moved sinusoidally over a white background (frequency 0.1Hz, illuminance 400 Lux).

4.4. OSCAR visual sensor for fixation and tracking

To illustrate the potential use of an OSCAR sensor, we built a miniature twin-engine aircraft, the body of which is about the size of a Khepera robot (Figure 7a). This microrobot, which is tethered to a 2m-long thin wire secured to the ceiling of the laboratory, orients in yaw by means of its two (differentially controlled) propellers. It is made of carbon, wood, fiberglass, and EPS. It weighs only 100g, including the engines and gears, the propellers, the scanning sensor (with its own position servo-system) and the complete electronics made with Surface Mounted Devices (SMD). The onboard rechargeable battery (LiMnO2, 9V-0.8A.h) adds another 54g, giving an endurance of 60 minutes.

Visual stabilization of micro-air-vehicles is still in its infancy. Ichikawa et al. were the first to achieve hover flight on a freely flying micro-helicopter [12]. They concluded that the resolution of the visual sensor is a crucial parameter which needed to be improved for achieving visual stabilization (hover was effective during 20 seconds only). Section 4.3 showed that retinal microscanning can help a visual system to improve its resolution. We therefore achieved the visual stabilization of the OSCAR robot by implementing a visual position servo-loop based on the OSCAR sensor [6]. The visual feedback loop acts so as to control the orientation of the robot around its yaw axis. As a consequence, the robot remains visually locked onto the target (edge or bar) placed in its Field Of View (FOV). As shown in Figure 7b, if the contrasting feature that is being fixated (an edge placed at 1.3m) happens to move, the robot responds with smooth pursuit. During this tracking episode, the robot pursued the target smoothly at yaw speeds of up to 20°/s.

5. CONCLUSION

Here we have described two Automatic Flight Control Systems that were developed at our laboratory to perform visual guidance of a Micro-Air Vehicle (MAV). First, we showed how a micro-aerial robot (OCTAVE) is able to control its lift to keep clear from the ground, despite moderate changes in the relief. This simple "optic flow servoing system" always makes sure that the robot keeps a safe distance from the ground – a distance which is beautifully adapted to its speed, whatever the speed. Secondly, we showed how a micro-scanning process helped to detect and locate contrasting features to a high accuracy, stabilize a MAV (OSCAR) around its yaw axis and have it track a moving feature.

Both studies, combined with previous laboratory studies [4], illustrate how an active visual process [25] can help an artificial flying agent to perceive the environment and achieve increasingly complex behaviors such as terrain avoidance and tracking. In the case of OCTAVE (section 3), active perception results from a purely translational motion during forward flight of the robot. In the case of OSCAR (section 4), active perception results from a purely rotational motion brought about by the scanning process. In both cases, however, optical *motion detection* is the sole cue which is used to extract a useful signal from the environment.

The EMDs can still be largely miniaturized so as to incorporate an array of pixels covering a much larger FOV, while keeping the excellent overall properties observed here in the robots:

- OCTAVE: robustness to randomly arranged contrasts and reproducibility of smooth terrain following,

without the occurrence of any crashes.

- OSCAR : invariance to contrast (from 10% to 90%) and distance (50cm to 2.5m), *minimum visibile* (8% of $\Delta\varphi$) and hyperacuity (2.5% of $\Delta\varphi$).

Our "biomimetic signal processing" approach has led us to develop smart autonomous flying machines that rely heavily on insect know-how and little on computer assisted resources. The biological models used in this study have been tested for 100 million years. They can provide an alternative when conventional stabilization and guidance systems fail to meet the draconian constraints imposed on vehicles such as MAVs, whose avionic payload will have to be expressed in grams or milligrams. However, the very principles used in our bio-inspired robots could also be adapted to the visual guidance of larger vehicles designed in the fields of aeronautics, aerospace and planetary exploration.

Acknowledgments

We thank Marc Boyron for his expert technical assistance and Jessica Blanc for improving the English manuscript. This research was supported by CNRS (Life Science, Engineering Science, Communication and Information Science and Technology, Cogniscience, Microsystem and Microrobotic Programmes) and by an EU contract (IST/FET - 1999- 29043).

References

[1] J-M. Pichon, C. Blanes and N. Franceschini, "Visual guidance of a mobile robot equipped with a network of self-motion sensors", Mobile Robots IV (Eds. W.J. Wolfe and W.H. Chun) Proc. S.P.I.E. 1195, Bellingham, U.S.A., pp. 44-53, 1989.

[2] N. Franceschini, J-M. Pichon and C. Blanes, "From insect vision to robot vision", Phil. Trans. Royal. Soc. B, 337:283-294, 1992.

[3] F. Mura and N. Franceschini, "Visual control of altitude and speed in a flying agent", From Animals to Animats III, D. Cliff et al. (eds.), pp. 91-99. MIT Press, 1994.

[4] F. Mura, N. Martin, and N. Franceschini "Biologically-inspired eye movements for the visually-guided navigation of mobile robots", Proc. Europ. Symposium. Artificial. Neural. Networks (ESANN), M. Verleysen (Ed.), D-Facto, Brussels, Belgium, pp. 135-147, 1996.

[5] S. Viollet and N. Franceschini, "Biologically-Inspired Visual Scanning Sensor for Stabilization and Tracking", Proc. of IEEE Conference on Intelligent Robots and Systems (IROS), Kyongyu, Corea, 1999.

[6] S. Viollet and N. Franceschini, "Visual servo system based on a biologically-inspired scanning sensor", SPIE Conf. on Sensor fusion and decentralized control in Robotics II, vol. 3839, pp. 144-155, 1999.

[7] T. Netter and N. Franceschini, "Neuromorphic Optical Flow Sensing for Nap-of-the-Earth flight", Mobile Robots XIV. SPIE Vol. 3838, Bellingham (Wa), U.S.A., pp. 208-216, 1999.

[8] T. Netter and N. Franceschini, "A Robotic Aircraft that Follows Terrain Using a Neuromorphic Eye", Proc. of IEEE Conference on Intelligent Robots and Systems (IROS), Lausanne, pp. 129-134, 2002.

[9] F. Ruffier, S. Viollet, S. Amic and N. Franceschini, "Bio-inspired optical flow circuits for the visual guidance of Micro-Air Vehicles", Proc. of IEEE International Symposium on Circuits and Systems (ISCAS), Bangkok, Thailand, 2003 (In Press).

[10] F. Ruffier and N. Franceschini "OCTAVE, a bioinspired visuo-motor control system for the guidance of Micro-Air-Vehicles", SPIE Conf. on Bioengineered and Bioinspired Systems, Maspalomas, Gran Canaria, Spain, Vol. 5119-2, 2003 (In Press).

[11] F. Iida, "Goal-directed navigation of an autonomous flying robot using biologically inspired cheap vision", 32nd Int. Symp. on Robotics, 19-21 April 2001.

[12] M. Ichikawa, H. Yamada and J. Takeuchi, "Flying robot with biologically inspired vision", Journal of Robotics and Mechatronics, 13:621-624, 2001.

[13] M.V. Srinivasan, S.W. Zhang, J. Chahl, E. Barth and S. Venkatesh, "How Honeybees make grazing landings on flat surfaces", Biological Cybernetics, 83, 3, 171-183, 2000.

[14] T.R. Neumann and H. Bülthoff, "Insect inspired visual control of translatory flight", ECAL 2001, pp 627-636. Springer-Verlag, 2001.

[15] G.L. Barrows, "Future visual microsensors for mini/micro-UAV applications", 7th IEEE International Workshop on Cellular Neural Networks and their Applications, 2002.

[16] T. Collett, H. Nalbach and H. Wagner, "Visual stabilization in arthropods", Visual Motion and its Role in the stabilization of Gaze, F.A. Miles, J. Wallman (eds.), pp. 239-263, Elsevier, 1993.

[17] W. Reichardt and R. Poggio, "Visual control of orientation behavior in the fly", Quarterly Reviews of Biophysics, 9 (3), 311-375, 1976.

[18] K. Hausen, "The lobula-complex of the fly : structure, function and significance in visual behaviour", Photoreception and Vision in Invertebrates, M. A. Ali (eds.), pp 523-559, New York: Plenum, 1984.

[19] N. Franceschini, C. Blanes and L. Oufar, "Passive, non-contact optical velocity sensor" (in French), Dossier technique ANVAR/DVAR N°51 549, Paris, 1986.

[20] N. Franceschini, A. Riehle and A. Le Nestour, "Directionally Selective Motion Detection by Insect Neurons", Facets of vision, D.G. Stavenga, R.C. Hardie (eds.), pp. 360-390. Berlin, Springer, 1989.

[21] J. S. Kennedy, The migration of the desert locust. Phil. Trans. Royal Soc. B 235:163-290, 1951.

[22] N. Franceschini and R. Chagneux, "Repetitive scanning in the fly compound eye," Proc. 25th Göttingen Neurobiology Conf., Elsner and Wässle, Eds., pp. 279, 1997.

[23] K.G. Götz, "Die optischen Übertragungseigenschaften der Komplexaugen von Drosophila", Kybernetik 2, 215-221, 1965.

[24] G. Westheimer, "Visual hyperacuity", Prog. Sensory Physiol. 1:1-37, 1981.

[25] Y. Aloimonos, "Visual Navigation", Lawrence Erlbaum Associates (Publishers), Mahwah (New Jersey), USA, 1997.